FreeSN: A Freeform Strut-node Structured Modular Self-reconfigurable Robot - Design and Implementation

Yuxiao Tu[1,2], Guanqi Liang[1,2], and Tin Lun Lam[1,2,†]

***Abstract*— This paper proposes a novel freeform strut-node structured modular self-reconfigurable robot (MSRR) called FreeSN, consisting of strut and node modules. A node module is mainly a low-carbon steel spherical shell. A strut module contains two freeform connectors, which provide strong magnetic connections and flexible spherical motions. The FreeSN system shares the benefits of freeform connection and strut-node structures. The freeform connection brings good adaptability to the environment. The triangle substructures inside the system configuration significantly improve the structural stability. The parallel execution of module motions can superpose the module capabilities and makes the system more scalable. The modules can combine these robot features by selecting the system configuration and better fit different circumstances and tasks. Four demonstrations, including assembly, obstacle crossing, transportation, and object manipulation, are designed to show the capabilities of the FreeSN system in different aspects. The results show the great performance and versatility of this MSRR system.**

Fig. 1. A freeform strut-node structured MSRR system - FreeSN.

I. INTRODUCTION

Modular self-reconfigurable robotic (MSRR) systems [1]–[5] consist of many repeated modules, which can rearrange themselves into different configurations, in order to adapt to different circumstances and perform different tasks. The previous MSRR modules are challenging to construct a large-scale and adaptable robotic system since the connector brings physical constraints or the system topology is not well scalable.

The connector is a crucial component of the MSRR system, providing the self-reconfiguration ability and deciding the system rigidity. Many types of creative connectors have been designed in the past decades. For example, the latches [6], [7] and hooks [8], [9] that are driven by shape memory alloys (SMA) or DC motors, electromagnet [10], and permanent magnets [11]–[13]. The connector has two important critical metrics: the area of acceptance [14] and connection strength. The area of acceptance decides the difficulty and success rate of the connecting process. The connection strength contributes to the module capability and system stability. The latches and hooks-based connectors always have strong connection strength but have a small area of acceptance, limiting the connection speed and success rate. The connectors based on electromagnet or permanent magnets always have a larger area of acceptance since the magnetic attraction requires no contact. However, the magnetic attraction is axial, limiting the connection strength in shear. Many previous magnetic connectors are gendered since the magnets are polarized, which brings certain configuration planning constraints.

A kind of connector has started to emerge, the freeform connector. The freeform connector has a large area of acceptance and generally has a continuous and more flexible connection. The MSRR with such connectors can better adapt to unstructured and dynamic environments. The early freeform connectors [15]–[17] are designed in 2D, but they have weak connections. Two 3D freeform MSRRs are proposed in recent years: FreeBOT [18] and FireAnt3D [19]. FreeBOT uses a permanent magnet connector, and a module can reconfigure on other modules freely. However, each FreeBOT module has only one connector, which brings certain topological stability constraints. FireAnt3D can generate strong and continuous connections by melting and cooling plastic, but the time and the power cost of the docks are high.

The MSRR system connection topology is an important issue that contributes to the stability and scalability of the robot system. The system connection topology can be roughly evaluated by two metrics: the maximum number of modules connected to one module and the minimum central angle between two connectors. Many previous MSRR modules are cubical and have at most six fixed-point connectors. However, the minimum central angle is 90 degrees, and the connection topology cannot contain triangles. This topological deficiency limits the scalability of these MSRR systems. More connectors can be integrated into the systems, but the additional weight, volume, and manufacturing cost can be ex-

This work was supported by the National Natural Science Foundation of China (62073274), and the funding AC01202101103 from the Shenzhen Institute of Artificial Intelligence and Robotics for Society.

[1] School of Science and Engineering, The Chinese University of Hong Kong, Shenzhen.
[2]Shenzhen Institute of Artificial Intelligence and Robotics for Society.
[†]Corresponding author is Tin Lun Lam tllam@cuhk.edu.cn

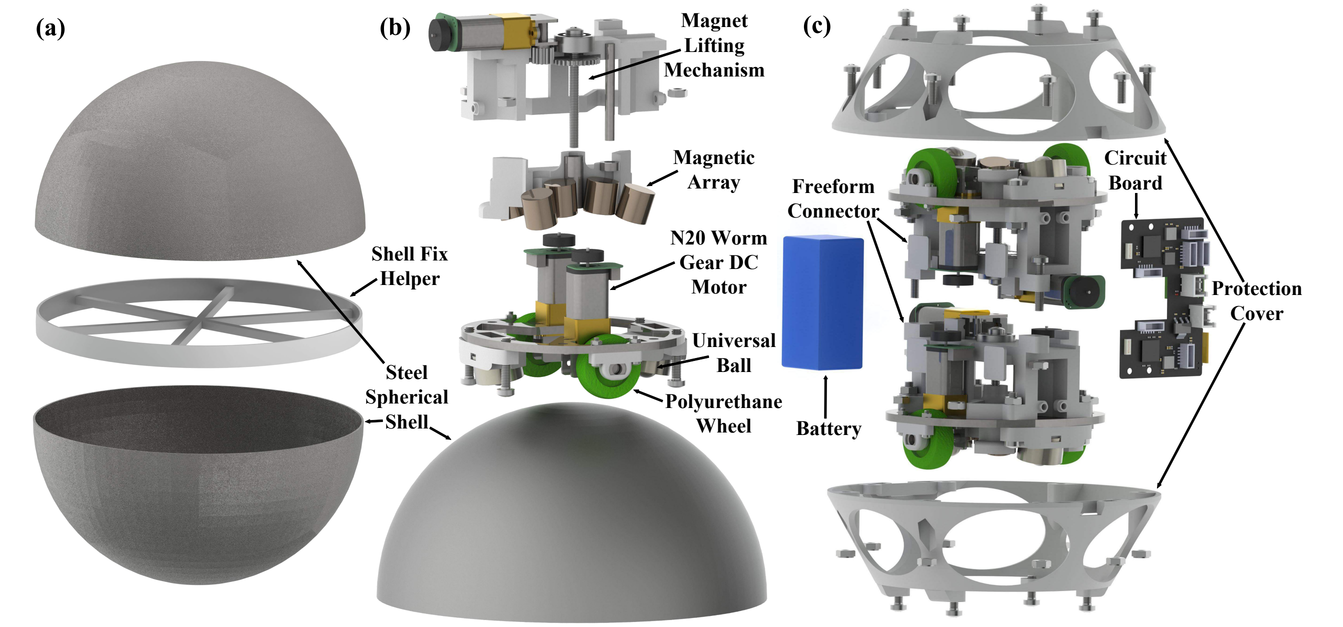

Fig. 2. The mechanism design of the FreeSN modules. (a) Node module. Exploded view. (b) Freeform Connector. Exploded view. Partial section view. (c) Strut module. Exploded view.

pensive. The truss is a widely used structure in buildings with excellent topological stability, assembled by two-force struts and nodes. A truss building always contains interconnecting triangles, which gives it the strength to withstand large dynamic loads both in compression and tension. Some early modular robot systems [20], [21] were designed as the truss structure, and the systems show good topological stability and scalability. However, they are not self-reconfigurable. A recent MSRR called Variable Topology Truss (VTT) [22] is proposed. It can change the structure topology with a gendered connector. However, the connector has a small area of acceptance, which brings a considerable motion constraint when changing the topology.

This paper proposes a novel freeform MSRR called FreeSN, consisting of strut and node modules. A node module is mainly a low-carbon steel spherical shell, and we propose a freeform magnetic connector, which has a large area of acceptance and strong connection strength. The connector can connect to any point of the node module without accurate alignment, continually reconfigure on the node module, and disconnect from the node module without manual assistance. A strut module contains two freeform connectors, and the modules can form a strut-node structured MSRR system. The FreeSN modules can cluster together and self-reconfigure to a strut-node structured configuration. The configuration can include parallel manipulator substructures, which can superpose the module capabilities and improve the system stiffness. It can also include triangle substructures, which can significantly improve the structural stability. The modules can consecutively change the configuration, balance the system adaptability and stability, and better fit into the new circumstances and tasks. The demonstrations show the great performance and versatility of this MSRR system.

II. Mechanical Design

The FreeSN system consists of strut modules and node modules. A strut module consists of two freeform connectors, which can connect, disconnect from a node module, and move on a node module freely. The mechanical design of the node module, the freeform connector, and the strut module are described, and finally, the specifications of the proposed implementation are summarized.

A. Node Module

In the current design, a node module is just a spherical shell manufactured by two low-carbon steel hemisphere shells, as shown in Fig. 2 (a). The two hemisphere shells are assembled by fixing them to the fix helper with epoxy. Then, the edge of the two shells is polished until smooth.

The node modules are not designed to be individually mobile, as mobility does not contribute much to the motion of the robot system and introduces additional weight. In the future design, the node module will undertake functions such as magnetic configuration detection [23], ad-hoc networking node, and energy sharing.

B. Freeform Connector

The mechanical design of the freeform connector is shown in Fig. 2 (b). It consists of a permanent magnet array, a magnet lifting mechanism, and a two-wheel differential driver. The magnet array produces a strong axial connection, while the lifting mechanism makes the connection force variable, and the driver brings spherical freeform motion.

The magnetic attraction between the magnet array and the low-carbon steel spherical shell is mainly axial since the steel spherical shell is homogeneous, and this provides the possibility for freeform connection. The magnets are arranged tangent to the spherical surface of the node module in alternating patterns, which increases the magnetic attraction and reduces disconnection distance. The magnetic attraction between steel shell and magnet array is genderless so that the connector can connect to the arbitrary position of the node module.

The distance between the magnet array and steel spherical shell is called magnet height. A magnet lifting mechanism driven by a DC motor and a screw rod is used to change the magnet height and adjust the magnetic attraction force so that the connector can connect to or disconnect from the node module. When the magnet height approaches zero, the magnetic force reaches its maximum. The connector can disconnect from the node module by lifting the magnets until the magnetic attraction is small enough.

The lifting mechanism can keep pushing the magnet after the magnet height approaches zero, where the magnet array contacts the steel spherical shell and the wheels are not. The magnet height is regarded negatively in this state. The magnet surface friction is relatively small, and the strut length is variable. We do not aim to create a linear actuated strut in this design because the difficulty is to make the connection strong but with a small central angle between two connectors. Although the actuation distance is small in this design, this motion still provides some powerful functions, and it can be easily improved in future designs if needed. For example, the magnet array can touch the external environment and generate a large thrust. The area of acceptance can also be improved in this way.

Since the magnetic attraction force is mainly axial, a two-wheel differential driver can provide spherical freeform motion and improve the connection strength. The differential driver consists of two DC motors with worm gear reducers, two polyurethane wheels, and two universal ball-bearing casters. The polyurethane wheel deforms under magnetic attraction load until the two casters touch the spherical shell in the meantime. Then, the extra magnetic attraction load will be applied to the casters, which brings little additional friction. The friction on the two polyurethane wheels provides the freeform motion driving force and the resistance to the shear force, bending moment, and torsion, which are vital to the connector performance. In this way, the driver provides the spherical freeform motion by rotating the polyurethane wheels. The worm gear reducers and polyurethane wheel friction compensate for the lack of tangential magnetic attraction force.

C. Strut Module

As shown in Fig. 2 (c), a strut module contains two symmetrically placed freeform connectors so that a strut module can connect to two node modules simultaneously. A dual Espressif ESP32-PICO-D4 microcontrollers circuit board is designed for motor control, wireless communication, and internal sensing. The protection cover protects the motors and electronics from external forces. Sufficient space is reserved for future extensions such as environmental sensors.

D. Specifications

The FreeSN contains a lot of parameters, which can be optimized for different applications. Here, we present an implementation with good overall performances based on the following principles. First, the minimum central angle between two connectors should be less than $60°$ so that the robot modules can construct triangle substructures. This is vital for structural stability. Second, the connector should be as strong as possible, considering the weight of the modules. Third, the modules should have enough space to place environmental sensors and necessary electronics and power costs it brings for future extension.

Considering the above principles and the manufacturing difficulty, we designed the robot with the following specifications. The diameter of the spherical shell in the node module is $120\,\mathrm{mm}$, while the thickness is $0.8\,\mathrm{mm}$. The magnet array consists of eight cylindrical magnets with a diameter of $10\,\mathrm{mm}$ and a height of $10\,\mathrm{mm}$. Under such configurations, the minimum central angle between two connectors is exactly less than $60°$, and a node module can be connected by 12 strut modules simultaneously. The strut module and node module masses are $480\,\mathrm{g}$ and $220\,\mathrm{g}$. The robot specifications of the implementation are summarized in Table I.

TABLE I
SPECIFICATIONS OF FREESN

Specification	Value
Strut Module	
- Magnet Remanence	$1.47\,\mathrm{T}$ (N52)
- Magnet Size	D: $10\,\mathrm{mm}$, H: $10\,\mathrm{mm}$
- Magnet Number	8
- Magnet Height Range	$[-15\,\mathrm{mm}, 10\,\mathrm{mm}]$
- Driver Motor Rated Speed (No Load)	$20\,\mathrm{RPM}$ ($12\,\mathrm{V}$)
- Lifting Mechanism Rated Speed (No Load)	$0.67\,\mathrm{mm\,s^{-1}}$ ($12\,\mathrm{V}$)
- Polyurethane Wheel Diameter	$20\,\mathrm{mm}$
- Caster Ball Diameter	$8\,\mathrm{mm}$
- Module Height	$77\,\mathrm{mm}$
- Module Weight	$480\,\mathrm{g}$
- Cost	$90 USD
Node Module	
- External Diameter	$120\,\mathrm{mm}$
- Thickness	$0.8\,\mathrm{mm}$
- Module Weight	$220\,\mathrm{g}$
- Cost	$2 USD

III. CONNECTOR CHARACTERIZATION

In this section, the magnet performance and the connection strength are preliminarily evaluated.

Fig. 3 shows the variation of the axial magnetic force with the magnet height, which contains the COMSOL Multiphysics simulation results and some real experimental results. The axial magnetic force is average $160\,\mathrm{N}$, where the magnetic attraction approaches its maximum. When the magnet height approaches $8\,\mathrm{mm}$, the magnetic force is less than 1% of its maximum, which is negligible. A connector could disconnect by the driving force of the other connector of the module when the magnet height is larger than $3\,\mathrm{mm}$,

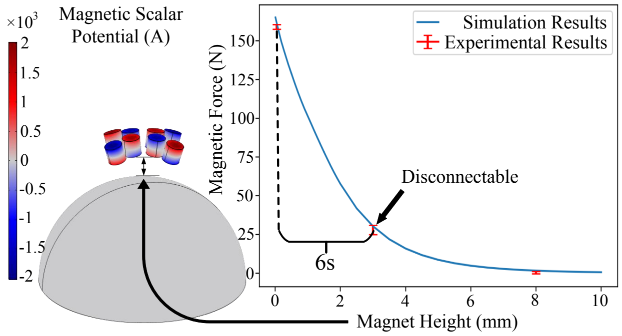

Fig. 3. Axial magnetic attraction force. The relationship between the magnetic force and the magnet height is presented, containing simulation data and experimental results. A simulation sample result is presented on the left side, which shows the magnetic scalar potential.

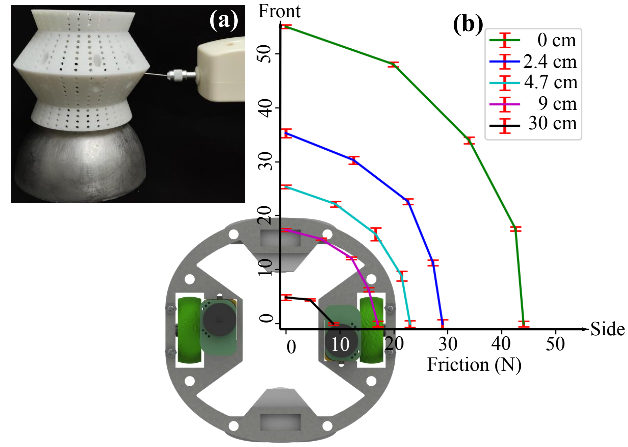

Fig. 4. Shear and bending strength test. (a) The forces is measured with a tensiometer and a 3D printed helper. (b) The shear and bending strength test results in different directions.

where the magnetic attraction is less than $30\,\mathrm{N}$. It takes about 6 seconds from the maximum connection force state to the disconnectable state. This process decides the minimum disconnect time, and it can be improved by using a more powerful actuator or increasing the supply voltage.

The connection strength can be characterized by normal strength, shear strength, bending strength, and torsional strength. The maximum magnetic attraction is about $160\,\mathrm{N}$, representing the normal strength. In real experiments, the connector is more susceptible to sliding due to shear force and bending moment created by gravity. The two strengths are not axisymmetric, caused by the distribution of the wheels. Under maximum magnetic force, we evaluated the shear strength and torque strength of the connector in several different directions. Five trials are performed in different directions and on different bending arms, with the 3D-printed helper shown in Fig. 4 (a). Under pure shear force, the maximum shear force is about $45\,\mathrm{N}$ in the side direction, while it is about $55\,\mathrm{N}$ in the front direction. When the bending arm increases to $9\,\mathrm{cm}$, the shear strength is nearly the same in all directions. The shear strength in the side direction is far stronger than in the front direction when the bending arm increases to $30\,\mathrm{cm}$. The maximum bending moment is approximately $1.5\,\mathrm{Nm}$ in the front direction and larger in the side direction. The experimental results are concluded in Fig. 4 (b). The torsional strength is tested similarly. When only torsion is applied, the maximum torsion is about $1.5\,\mathrm{Nm}$.

Since the gravities of the strut and node modules are $4.7\,\mathrm{N}$ and $2.16\,\mathrm{N}$, and the lengths are $7.7\,\mathrm{cm}$ and $12\,\mathrm{cm}$. It is equivalent to supporting about 2.8 modules as a cantilever. The overall connection strength is good compared with the previous fixed-point magnetic connectors.

IV. Motion of The FreeSN System

A. Individual Motion

Each strut module have six actuators, and the individual motions are summarized based on functionality as follows:

- *Connect*: A strut module connects to a node module by reducing the magnet height. The magnet height can be adjusted in advance for fast connection.
- *Disconnect*: A strut module disconnects from a node module by increasing the magnet height until the magnetic attraction is small enough.
- *Slide*: A strut module moves on the node module.
- *Spin*: The two drivers of a strut module rotate in the same direction simultaneously.
- *Drive*: When the rubber tire contacts external environments such as the ground, it can rotate and provide the driving force.
- *Lift*: The strut can work as a linear actuator or generate thrust to the external environments using the magnet lifting mechanism.

B. Parallel Motion

Benefitting from the strut-node structure and freeform connector, the individual motions of strut modules can be highly parallelized. The parallel motions of the FreeSN system can be roughly divided into three categories: the motion of truss structured parallel manipulator, multi-module cooperative motion, and the combination of the first two. The parallel motions make the robot system more scalable.

A parallel manipulator can be achieved as the truss structures, which were studied in [20]–[22] using linear actuated struts and passively actuated spherical joints. The FreeSN modules can form the parallel manipulator in the same way, with the difference that the spherical joints are actuated. Our parallel manipulator can move as the previous modular parallel manipulator with a short linear actuation distance. The manipulator can also move using only actuated spherical joints, which is more efficient for this robot. This type of motion relies on the closed-loop strut-node structures. The structure will constrain the individual motion of each module and improve the system stiffness. Fig. 5 (a) shows a deformable cube. The motion of individual motion is constrained by the quadrangle substructures, and any deformation requires the parallel motion of at least four modules.

Different from the parallel manipulator, multiple strut modules can cooperate to finish some motions, where a

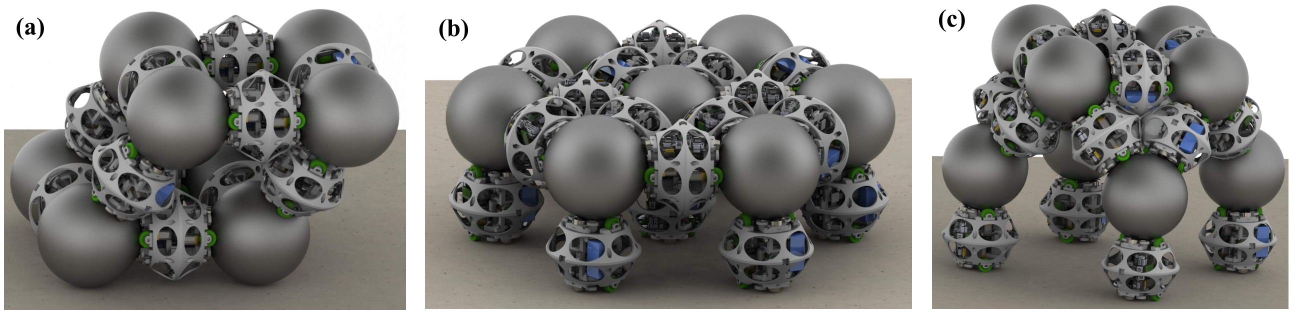

Fig. 5. Example configurations for the three types of parallel motion. (a) A deformable cube. (b) A fourteen-wheel truck. (c) A quadruped robot.

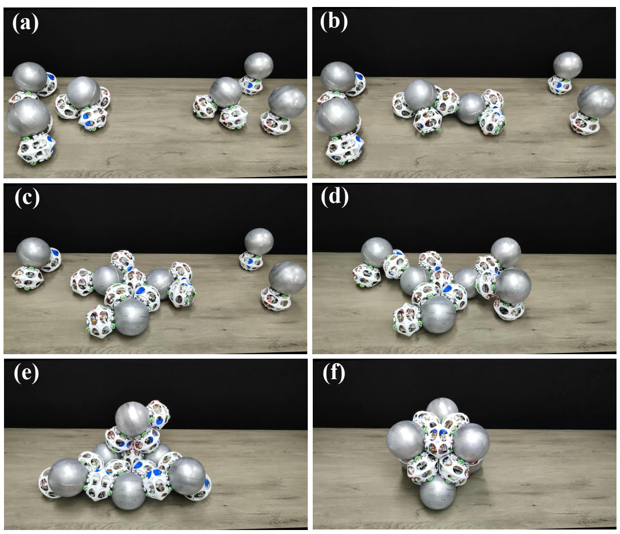

Fig. 6. Assembly. The modules cross together and construct an octahedron.

module will not constrain the motion of other modules. For example, modules can move as a wheeled robot as shown in Fig. 5 (b). The robot can move when most strut modules cooperate well, but some modules can be uncooperative, and there are no strict mechanical constraints for each module.

Fig. 5 (c) shows a example of the hybrid parallel motion. The modules form a quadruped robot. Each leg includes a triangle parallel manipulator, while the motions of the four legs are cooperative.

V. Experimental Results

We demonstrate the capabilities of the FreeSN system in different tasks, i.e., 1) assembly, 2) obstacle crossing, 3) transportation, 4) object manipulation, which shows the features and performance of FreeSN in different aspects. A maximum number of thirteen strut modules and seven node modules are used, which are manually controlled to finish the tasks.

A. Assembly

This task shows a self-assembly process of the FreeSN system. As shown in Fig. 6, a node module and one to three strut modules form a unit initially. The six units cluster together as wheeled robots, connect to each other, and finally reconfigure to an octahedron truss configuration. Such configuration is structurally stable since it contains many triangle substructures.

B. Obstacle Crossing

As shown in Fig. 7, the modules start from an octahedron truss configuration and aim to cross the gully. The modules cross the gully by consecutive self-reconfigurations. There are only twelve strut modules can six node modules, so the center of mass of the system is sometimes difficult to stabilize and requires some additional motions to keep it stable. Finally, all modules successfully cross the gully.

The self-configuration is achieved by two strategies in this demonstration. First, one node module and two to three strut modules can form a unit, and such a unit can reconfigure on any stable structures that consist of FreeSN modules. A larger scale of parallel motion in this pattern is more complex but achievable. Second, a single strut module can possibly freely reconfigure on the structures where other strut modules need to make way for it. This is a valuable strategy when too many redundant strut modules exist, or the center of gravity is unstable.

C. Transportation

The modules form a quadrupedal wheeled robot as the initial configuration, which aims to transport a table with books. As shown in Fig. 8, the quadrupedal wheeled robot stands up and moves under the table as a wheeled robot through the parallel *Drive* motion. Then, it lifts the table through the parallel *Lift* motion of the strut modules, transports the table, and puts the table down.

In this task, the thirteen strut modules and four node modules weigh $7.1\,\mathrm{kg}$, and they successfully transport $22.8\,\mathrm{kg}$ of books. Although $22.8\,\mathrm{kg}$ is far from the theoretical load limit, the experimental result is satisfying. This kind of parallel motion can be easily extended.

D. Object Manipulation

In this task, nine strut modules and six node modules construct a parallel manipulator, as shown in Fig. 9. The parallel *Slide* motion of the three middle strut modules decides the pose of the upper triangle so that the box can be manipulated. The manipulator moves the box horizontally

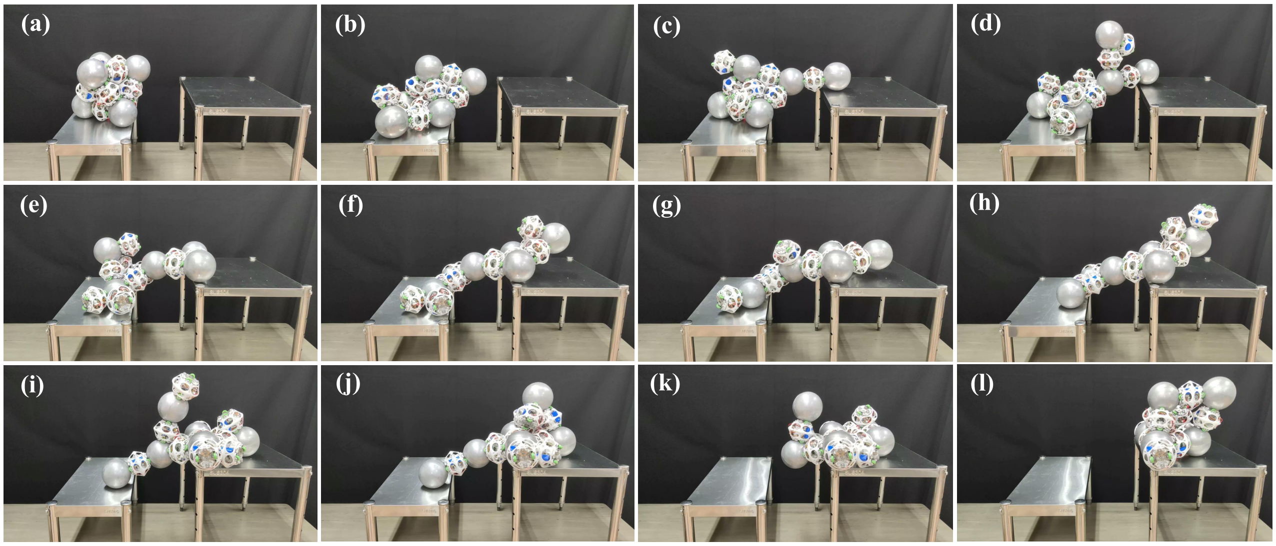

Fig. 7. Obstacle crossing. The modules cross a gully consisting of two tables by consecutive self-reconfigurations.

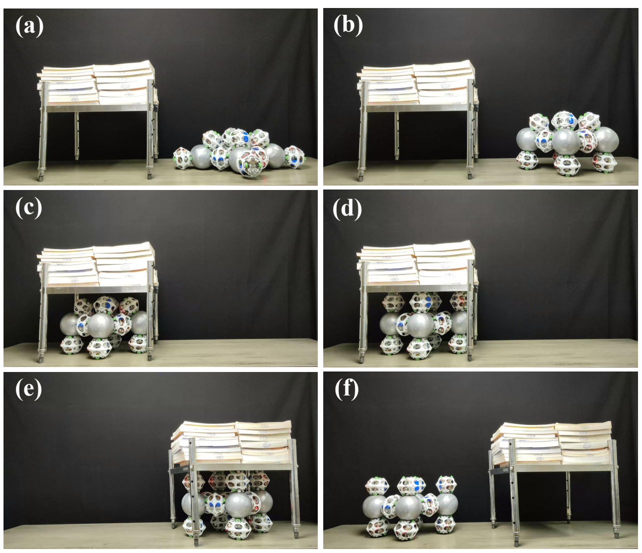

Fig. 8. Transportation. The modules transport a table with books as a wheeled robot.

from the table on the left to the one on the right, then pushes it to the table in another configuration.

This demonstration mainly shows the performance of such a redundant parallel manipulator. The system topology makes the manipulator more stable than the chain configuration. The superposition of redundant actuators also provides a larger manipulation payload.

VI. CONCLUSIONS AND FUTURE WORK

This paper proposes a novel MSRR called FreeSN, a strut-node structured system with freeform connectors. The freeform connector brings the spherical freeform connection between the strut and node modules, which gives the system better adaptability to the environments. The connection strength is strong in normal and good in shear and torque

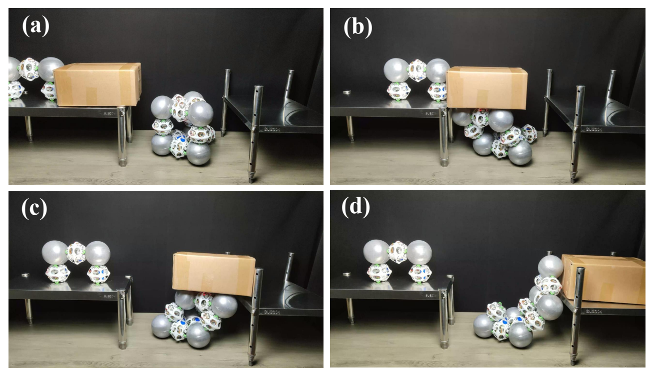

Fig. 9. Object manipulation. The modules manipulate the box as a parallel manipulator.

for individual freeform motion. However, the connection strength and actuator torque are not enough for some large-scale tasks, which can be improved by parallel motion. The strut-node structures make the strut motions easier to be parallelized. The modules can form parallel manipulator substructures, which can superpose the actuator torques. The modules can also form triangle substructures, significantly increasing the structural stability. The parallel motion and structural stability are the most significant features for the FreeSN towards a large-scale and versatile MSRR system. The demonstrations show the great performance and versatility of the FreeSN MSRR system.

Future work on the FreeSN system will focus on three aspects. First, the robot parameters can be further optimized for better overall performance and lower manufacturing costs. Second, we aim to build an MSRR system without external sensors. Thus, magnetic configuration detection and identification systems are necessary for future automation. Third, parallel motion is a significant issue of this wirelessly connected MSRR system. A distributed parallel motion framework needs to be studied.

REFERENCES

[1] A. K. S. Sankhar Reddy Chennareddy, Anita Agrawal, "Modular self-reconfigurable robotic systems: A survey on hardware architectures," *Journal of Robotics*, vol. 2017, p. 1–19, 2017.

[2] M. Yim, W. Shen, B. Salemi, D. Rus, M. Moll, H. Lipson, E. Klavins, and G. S. Chirikjian, "Modular self-reconfigurable robot systems [grand challenges of robotics]," *IEEE Robotics Automation Magazine*, vol. 14, no. 1, pp. 43–52, 2007.

[3] J. Seo, J. Paik, and M. Yim, "Modular reconfigurable robotics," *Annual Review of Control, Robotics, and Autonomous Systems*, vol. 2, no. 1, pp. 63–88, 2019. [Online]. Available: https://doi.org/10.1146/annurev-control-053018-023834

[4] A. Brunete, A. Ranganath, S. Segovia, J. P. de Frutos, M. Hernando, and E. Gambao, "Current trends in reconfigurable modular robots design," *International Journal of Advanced Robotic Systems*, vol. 14, no. 3, p. 1729881417710457, 2017. [Online]. Available: https://doi.org/10.1177/1729881417710457

[5] A. Hayat, "A framework for taxonomy and evaluation of self-reconfigurable robotic systems," *IEEE Access*, 01 2020.

[6] B. Salemi, M. Moll, and W. Shen, "Superbot: A deployable, multi-functional, and modular self-reconfigurable robotic system," in *2006 IEEE/RSJ International Conference on Intelligent Robots and Systems*, 2006, pp. 3636–3641.

[7] A. Spröwitz, S. Pouya, S. Bonardi, J. V. Den Kieboom, R. Möckel, A. Billard, P. Dillenbourg, and A. J. Ijspeert, "Roombots: Reconfigurable robots for adaptive furniture," *IEEE Computational Intelligence Magazine*, vol. 5, no. 3, pp. 20–32, 2010.

[8] M. W. Jorgensen, E. H. Ostergaard, and H. H. Lund, "Modular atron: modules for a self-reconfigurable robot," in *2004 IEEE/RSJ International Conference on Intelligent Robots and Systems (IROS) (IEEE Cat. No.04CH37566)*, vol. 2, 2004, pp. 2068–2073 vol.2.

[9] H. Wei, Y. Chen, J. Tan, and T. Wang, "Sambot: A self-assembly modular robot system," *IEEE/ASME Transactions on Mechatronics*, vol. 16, no. 4, pp. 745–757, 2011.

[10] V. Zykov, E. Mytilinaios, M. Desnoyer, and H. Lipson, "Evolved and designed self-reproducing modular robotics," *IEEE Transactions on Robotics*, vol. 23, no. 2, pp. 308–319, 2007.

[11] J. W. Romanishin, K. Gilpin, S. Claici, and D. Rus, "3d m-blocks: Self-reconfiguring robots capable of locomotion via pivoting in three dimensions," in *2015 IEEE International Conference on Robotics and Automation (ICRA)*, 2015, pp. 1925–1932.

[12] J. Davey, N. Kwok, and M. Yim, "Emulating self-reconfigurable robots - design of the smores system," in *2012 IEEE/RSJ International Conference on Intelligent Robots and Systems*, 2012, pp. 4464–4469.

[13] T. Tosun, J. Davey, C. Liu, and M. Yim, "Design and characterization of the ep-face connector," in *2016 IEEE/RSJ International Conference on Intelligent Robots and Systems (IROS)*, 2016, pp. 45–51.

[14] N. Eckenstein and M. Yim, "Area of acceptance for 3d self-aligning robotic connectors: Concepts, metrics, and designs," in *2014 IEEE International Conference on Robotics and Automation (ICRA)*, 2014, pp. 1227–1233.

[15] M. Shimizu, T. Mori, and A. Ishiguro, "A development of a modular robot that enables adaptive reconfiguration," in *2006 IEEE/RSJ International Conference on Intelligent Robots and Systems*, 2006, pp. 174–179.

[16] H. Tokashiki, H. Amagai, S. Endo, K. Yamada, and J. Kelly, "Development of a transformable mobile robot composed of homogeneous gear-type units," in *Proceedings 2003 IEEE/RSJ International Conference on Intelligent Robots and Systems (IROS 2003) (Cat. No.03CH37453)*, vol. 2, 2003, pp. 1602–1607 vol.2.

[17] J. Campbell, P. Pillai, and S. Goldstein, "The robot is the tether: active, adaptive power routing modular robots with unary inter-robot connectors," in *2005 IEEE/RSJ International Conference on Intelligent Robots and Systems*, 2005, pp. 4108–4115.

[18] G. Liang, H. Luo, M. Li, H. Qian, and T. L. Lam, "Freebot: A freeform modular self-reconfigurable robot with arbitrary connection point - design and implementation," in *2020 IEEE/RSJ International Conference on Intelligent Robots and Systems (IROS)*, 2020, pp. 6506–6513.

[19] P. Swissler and M. Rubenstein, "Fireant3d: a 3d self-climbing robot towards non-latticed robotic self-assembly," in *2020 IEEE/RSJ International Conference on Intelligent Robots and Systems (IROS)*, 2020, pp. 3340–3347.

[20] G. Hamlin and A. Sanderson, "Tetrobot: a modular system for hyper-redundant parallel robotics," in *Proceedings of 1995 IEEE International Conference on Robotics and Automation*, vol. 1, 1995, pp. 154–159 vol.1.

[21] A. Lyder, R. F. M. Garcia, and K. Stoy, "Mechanical design of odin, an extendable heterogeneous deformable modular robot," in *2008 IEEE/RSJ International Conference on Intelligent Robots and Systems*, 2008, pp. 883–888.

[22] A. Spinos, D. Carroll, T. Kientz, and M. Yim, "Variable topology truss: Design and analysis," in *2017 IEEE/RSJ International Conference on Intelligent Robots and Systems (IROS)*, 2017, pp. 2717–2722.

[23] Y. Tu, G. Liang, and T. L. Lam, "Graph convolutional network based configuration detection for freeform modular robot using magnetic sensor array," in *2021 IEEE International Conference on Robotics and Automation (ICRA)*, 2021, pp. 4252–4258.